Linking evapotranspiration seasonal cycles to the water balance of headwater catchments with contrasting land uses

Peixoto Neto, Alberto ML, Cartwright, Ian, Silva, Marcela RF, McHugh, Ian, Dresel, P Evan, Teodosio, Bertrand, Jovanovic, Dusan, McCaskill, Malcolm, Webb, John and Daly, Edoardo (2022) Linking evapotranspiration seasonal cycles to the water balance of headwater catchments with contrasting land uses. Hydrological Processes, 36 (12). ISSN 0885-6087

Received: 6 May 2022 | Revised: 9 December 2022 | Accepted: 10 December 2022

DOI: 10.1002/hyp.14784

WILEY

RESEARCH ARTICLE

Linking evapotranspiration seasonal cycles to the water balance of headwater catchments with contrasting land uses

Alberto M. L. Peixoto Neto[1] | Ian Cartwright[2] | Marcela R. F. Silva[1] | Ian McHugh[3] | P. Evan Dresel[4] | Bertrand Teodosio[5] | Dusan Jovanovic[6] | Malcom R. McCaskill[7] | John Webb[8] | Edoardo Daly[1]

[1]Department of Civil Engineering, Monash University, Melbourne, Victoria, Australia

[2]School of Earth, Atmosphere and Environment, Monash University, Melbourne, Victoria, Australia

[3]School of Ecosystem and Forest Sciences, The University of Melbourne, Melbourne, Victoria, Australia

[4]Department of Jobs, Precincts, and Regions, Agriculture Research Victoria, Bendigo, Victoria, Australia

[5]Institute of Sustainable Industries and Liveable Cities, Victoria University, Melbourne, Victoria, Australia

[6]Faculty of Civil Engineering, University of Novi Sad, Subotica, Serbia

[7]Agriculture Research Victoria, Hamilton, Victoria, Australia

[8]Environmental Geoscience, Department of Ecology, Environment and Evolution, La Trobe University, Melbourne, Victoria, Australia

Correspondence
Alberto M. L. Peixoto Neto, Department of Civil Engineering, Monash University, Clayton, Melbourne, VIC 3800, Australia.
Email: alberto.peixoto@monash.edu

Funding information
Australian Research Council, Grant/Award Numbers: LP140100871, DP180101229

Abstract

Land use affects evapotranspiration rates and is a primary driver of the catchment water balance. The water balance of two catchments in southeastern Australia dominated by either grazed pasture or blue gum (*Eucalyptus globulus*) plantation was studied, focusing on the patterns of evapotranspiration (ET) throughout the year. Rainfall, streamflow, and groundwater levels measured between 2015 and 2019 were combined to estimate annual ET using a water balance equation. In the pasture, eddy covariance was used to measure ET from the catchment. Sap flow measurements were used to estimate tree transpiration in May 2017–May 2018 and Feb 2019–Feb 2021 in two different plots within the plantation. The tree transpiration rates were added to interception, estimated as a percentage of annual rainfall, to calculate ET from the plantation catchment. ET in the pasture showed strong seasonal cycles with very low ET rates in summer and ET rates in spring that were larger than the transpiration rates in the plantation, where trees transpired consistently throughout the year. The estimated annual ET from the water balance equation was comparable to ET estimated from other measurements. In the pasture, ET on average accounted for 88% of annual rainfall, while ET in the plantation was on average 93% of rainfall, exceeding it in the years with annual rainfall lower than about 500 mm. The difference between the ET rates in the plantation and the pasture was approximately 30–50 mm y^{-1}. The larger ET rates in the plantation were reflected in a gradual decrease in the groundwater storage. The larger ET rates were enough to cause a decrease in groundwater storage in the plantation but not in the pasture, where groundwater levels remained stable.

KEYWORDS
catchment water balance, ephemeral streams, evapotranspiration, groundwater, intermittent rivers, pasture, plantation, recharge

1 | INTRODUCTION

Land use and land-use changes are recognized to affect water resources, determining the quantity and quality of streamflow and groundwater storage (Foley et al., 2005; Scanlon et al., 2007; Veldkamp et al., 2017). Afforestation and the establishment of commercial tree plantations, while providing benefits such as reduction of soil erosion and natural carbon sequestration, often cause reductions in the water yield which may lead to salt accumulation in the soil and groundwater (Gribovszki et al., 2017; Jackson et al., 2005; Nosetto et al., 2008). However, hydrological responses to land-use changes, their extent, and the mechanisms causing them are still poorly understood globally (van Dijk & Keenan, 2007; Zhang et al., 2007, 2017).

There is a general agreement that forests use more water and intercept more rainfall than short-rooted plants such as pasture grasses, and thus have lower streamflow and groundwater recharge rates (Benyon et al., 2006; Colville & Holmes, 1972; Dresel et al., 2018; van Dijk & Keenan, 2007). In Australia, a vast conversion of native forests into land for agricultural productivity, such as crops and pastures for livestock grazing, has occurred since the late 1800s (Barson, 2000; Bradshaw, 2012; Dregne, 2002). Following the large-scale replacement of native trees with grasses and crops, many catchments experienced an increase in groundwater recharge, which caused dryland salinity issues in drier regions of southern Australia or enhanced where pre-existing (Cartwright et al., 2004; Hatton et al., 2003; Jolly et al., 2001). Several national initiatives aimed to boost regional economic growth and tackle this issue through afforestation by fast-growing species (Prăvălie, 2016; Zhang et al., 2007). *Eucalyptus globulus* Labill. (Tasmanian blue gum) is one of the dominant tree species that was extensively planted in Australia (Downham & Gavran, 2020). In addition, the area known as the Green Triangle, across south of South Australia and western Victoria, experienced the establishment of large *E. globulus* plantations for commercial purposes (Downham & Gavran, 2020; Iglesias-Trabado et al., 2009). After the Millennium Drought, which affected southern Australia from about 1997–2009, groundwater levels decreased (Peterson et al., 2021; Van Dijk et al., 2013). This reduced the problems associated with dryland salinity, but raised concerns about the water availability in those catchments that were recently converted from pastures to commercial tree plantations.

Although paired catchment studies tend to show that afforestation is associated with a reduction in streamflow (e.g., Brown et al., 2005), which is attributed to the interception of rainfall and tree transpiration rates, recent studies in catchments with non-perennial streams showed that land use might not be the dominant factor affecting streamflow. For example, comparing the water balance of adjacent small headwater catchments dominated by pasture or plantations in southeast Australia, Dean et al. (2016) and Dresel et al. (2018) found that streamflow, occurring for a few months every year, was less affected by land use than the groundwater storage. Barua et al. (2021, 2022) concluded that the riparian zone was important in feeding non-perennial streams. These areas are not normally planted to plantation trees, and soil moisture is often high because of discharge from groundwater. This highlights the role of geological features in determining the groundwater recharge and the connectivity between subsurface and surface water. Dresel et al. (2018) concluded that evapotranspiration rates in Australian pastures were comparable to those in forested catchments in areas with average annual rainfall lower than approximately 600 mm. Some modelling studies have highlighted the importance of the location of planted and unplanted areas in generating streamflow (Azarnivand et al., 2020; Daneshmand et al., 2019; Niedda & Pirastru, 2014). A modelling study of streamflow in the Glenelg basin of Australia found that, at the regional scale, the establishment of plantations that are scattered in small catchments across the landscape did not have strong effects on total annual streamflow (Brown et al., 2015). Other modelling studies, however, suggest reduction of streamflow following the establishment or expansion of plantations (Brown et al., 2007; Herron et al., 2003; Li et al., 2012; Webb & Kathuria, 2012; Zhang et al., 2011, 2012).

Most of the experimental and modelling studies focused on precipitation and streamflow measurements to estimate annual changes in water yield (e.g., Brown et al., 2005) with other studies also using groundwater elevations, which are more difficult to obtain (Dresel et al., 2018; Niedda & Pirastru, 2014). Direct measurements of evapotranspiration or tree transpiration are less common, although these are important for constraining the water balance (Dean et al., 2015) and understanding the water stores that trees and grasses might use (Benyon et al., 2006; McCaskill et al., 2016; Thayalakumaran et al., 2018). Although representing a large component of evapotranspiration, evaporation of water intercepted by tree canopy and ground litter is often not measured. Measurements from Australia and Uruguay suggest that approximately 18 to 20% of rainfall can be intercepted by the tree canopy, with an additional 25%–30% intercepted by litter (Benyon & Doody, 2015; Silveira et al., 2016).

The objective of this study was to identify and quantify the differences in the evapotranspiration rates in two headwater catchments, one used as a pasture for grazing and the other largely covered by a blue gum plantation, to understand how these differences affected the water balance of the two catchments. This study builds on the work of Dresel et al. (2018), who estimated evapotranspiration rates from measurements of other components of the water balance in the same catchments in the period 2011–2016. Direct measurements of evapotranspiration rates in the pasture and sap flow in some trees in the plantation are used to better constrain the water balance in the period 2015–2019. Understanding the patterns and behaviour of water-use in common land-uses from dry regions can lead to more effective management of water resources.

2 | SITE DESCRIPTION

The study site consists of two catchments near Gatum in southwestern Victoria, Australia, about 300 km from Melbourne (Figure 1). One catchment, with a surface area of 151 ha, is predominantly a pasture (97%) with winter-active perennial grasses (*Phalaris aquatica L.* and *Trifolium subteraneum L.*) used for sheep and cattle grazing; the remaining

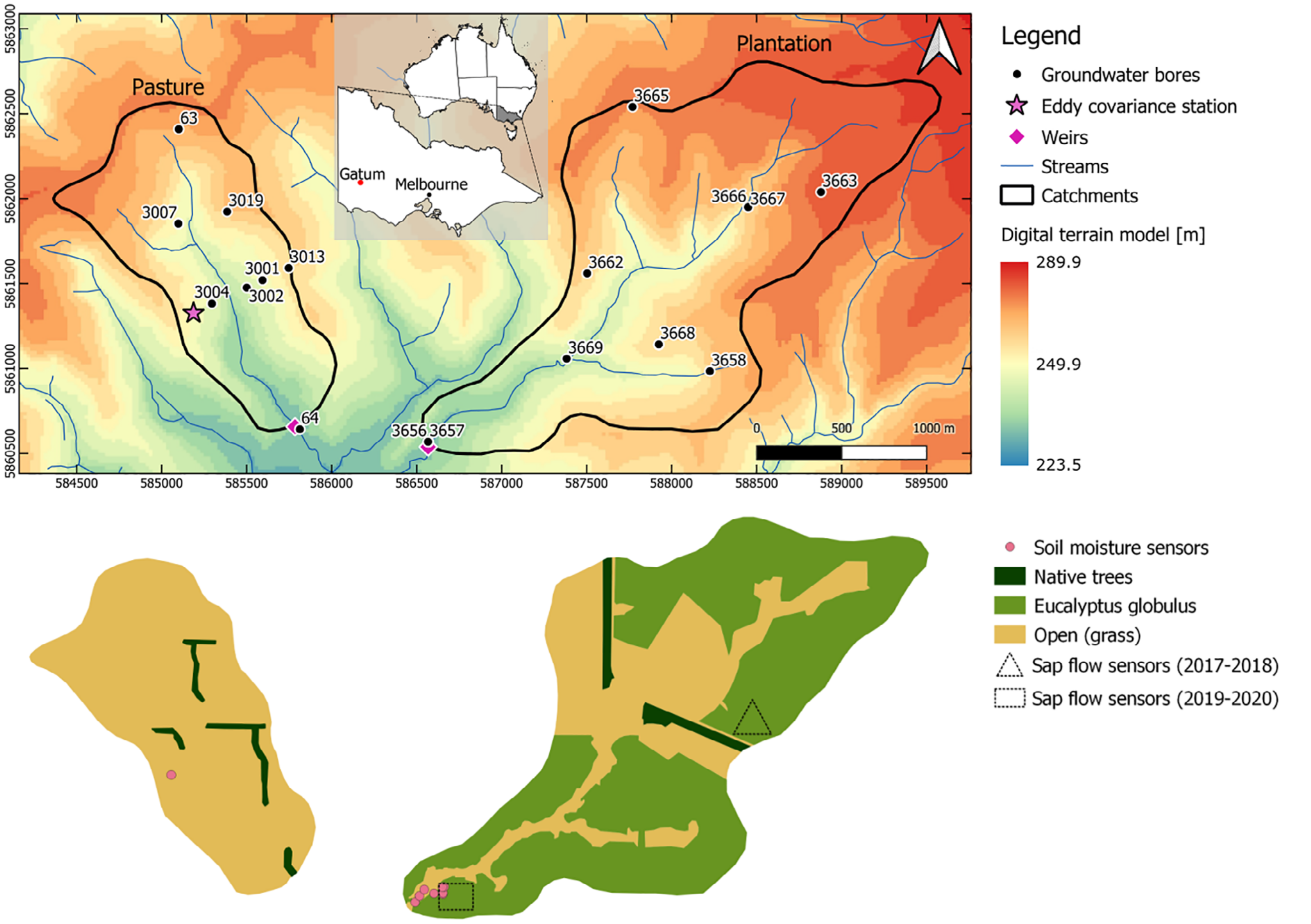

FIGURE 1 Top: Digital terrain model of the study site area with the two catchments boundaries: Pasture (left) and plantation (right). Groundwater bores and weirs are shown in both catchments with the location of the eddy covariance system in the pasture. Inset: Map of Australia highlighting the state of Victoria and showing the location of Gatum in Victoria. Bottom: Land use and location of soil moisture sensors in the catchments; in the plantation, the two different areas where sap flow was measured are also indicated

3% of the catchment area is covered by native trees. The other catchment, with a surface area of 338 ha, is predominantly covered by a *E. globulus* (blue gum) plantation. This was established in 2005 at a stocking density of about 800 trees ha^{-1} and has naturally thinned over time to about 730 trees ha^{-1} in 2015. Mean diameter at breast height (DBH) and mean height are about 24 cm and 20 m, respectively (Dresel et al., 2018). The plantation covers about 68% of the catchment excluding an irregular riparian buffer zone of 10–100 s of metres from the watercourse. The remaining areas in the plantation are covered by pasture, unplanted grass and some native trees. The two catchments have similar topography and are drained by small creeks (Banool Creek in the pasture and McGill Creek in the plantation), which flow consistently for a few months every year. In both catchments, soils in the valleys and lower slopes are higher in silt than the elevated areas, from the surface up to 40 cm depth. In deeper layers, at about 1 m depth, the soil is characterized by grey sandy clay (Adelana et al., 2015). The bedrock in both catchments is composed by rhyolitic ignimbrites formed during the Lower Devonian (Morand et al., 2003). More details about the soil and geology of the catchments and the surrounding area are described by Adelana et al. (2015), Dresel et al. (2018) and Barua et al. (2021).

The long-term average rainfall in the area is 596 mm per year (1960–2020), mostly occuring during winter, as per SILO (Scientific Information for Land Owners, available at www.longpaddock.qld.gov.au/silo) database (Jeffrey et al., 2001). SILO is an Australian dataset based on observations from the Bureau of Meteorology (BoM) that estimate missing data using spatial interpolation algorithms at a daily timestep (Jeffrey et al., 2001). The average annual pan evaporation is estimated at about 1400 mm (Adelana et al., 2015). The climate is classified as temperate, with dry and warm summers (Köppen-Geiger zone 'Csb') (Beck et al., 2018). In the period between 1984 and 2022, the highest temperatures occurred in January and February, with an average monthly maximum temperature of 24°C, while the lowest temperatures were generally in July, with a long-term average monthly minimum of 5.6°C (Jeffrey et al., 2001). The mean maximum temperature during winter (Jun–Ago) was about 13°C and the mean minimum temperature during summer (Dec–Feb) was about 11°C (Jeffrey et al., 2001).

3 | DATA AND METHODS

3.1 | Data collection and analysis

3.1.1 | Meteorological variables

Meteorological variables were collected in the pasture at the same location as the eddy covariance station (Figure 1). In 2015, net radiation was measured every 30 minutes with a net radiometer (Q7.1, Campbell Scientific, Logan, UT). From 2016 onwards, another net radiometer was used (CNR4, Kipps and Zonen, Delft, The Netherlands). This provided four radiant flux measurements, including downwelling shortwave radiation at 30-minute temporal resolution. Air temperature and relative humidity were measured by the HMP110 probe (Vaisala, Helsinki, Finland) from 2015 at 30-minute intervals, and were used to calculate vapour pressure deficit (VPD) following Buck (1981). Rainfall data in 2015 and 2016 was measured in the mid to high slope on the plantation catchment and available in Dresel et al. (2018). As measurements failed in the following years, the remaining years (2017–2019) were obtained from the SILO gridded dataset at the coordinates -37.40°, 142.00°; SILO data is based on the interpolation of records from the nearby stations. SILO estimates are highly correlated to the daily measurements in 2015 and 2016 ($R^2 = 0.91$). For the annual rainfall in 2011–2016, the slope of the least square fit between the data measured at the site and SILO estimates is 0.97, indicating a good agreement between the two datasets.

3.1.2 | Soil water content

Soil moisture data was recorded about 3 m south from the eddy covariance station in the pasture from 2015 through 2019, using water content reflectometers (CS616, Campbell Scientific Instruments, USA); measurements were taken every 30 min at nine different depths from the surface (5, 15, 30, 50, 70, 90, 107, 130, and 150 cm). In the plantation, eight soil moisture probes (Drill & Drop, Sentek) installed in 2019 measured soil water content every 30 min, at depths from 5 to 115 cm at 10 cm increments. These measurements, at 12 different depths, were taken in different locations within the catchment (Figure 1). Three probes were in the open area along the bank of McGill Creek, and five were installed in the plantation, three between plantation tree lines and two between trees along the same line. One of the probes closest to trees ('between trees') was disregarded from the analysis as it seemed to have detached from the soil, recording unreasonably dry values.

3.1.3 | Groundwater

A network of surveyed groundwater observation bores exists across the two catchments (8 bores in the pasture and 10 bores in the plantation, Figure 1). The total depth of the bores varied from 13 to 30 m in the pasture and 4 to 30.8 m in the plantation (Barua et al., 2021; Hekmeijer et al., 2011). Each bore was equipped with a data logger (Schlumberger diver or In-Situ AquaTroll data loggers) to record groundwater levels at 4 h intervals from 2009 or early 2010 through 2019. Correction for barometric pressure fluctuations were made from In-Situ BaroTroll logger installed at the site. Suspect data, comprised by mostly unreasonable spikes and data during sampling, were excluded. This was only about 0.02% of the data in the plantation since the end of 2017, following the measurements presented by Dresel et al. (2018). The groundwater elevations are presented as hydraulic heads (m) above Australia Height Datum (AHD).

3.1.4 | Streamflow

Streamflow at the outlet of the pasture catchment was measured with a triangular sharp-crested weir ('V-notch') and a rectangular broad-crested weir measured streamflow in the plantation (Hekmeijer et al., 2011). The water levels were recorded every 30 min by Campbell data loggers and converted to volumetric flow rates using a rating curve. Streamflow is divided by the respective catchment area to express streamflow in equivalent water depth (m) allowing its comparison with other variables of the water balance. As streamflow measurements in the plantation failed in 2018 and 2019, the annual streamflow in this catchment for these 2 years was estimated based on the relationship between annual streamflow and annual rainfall from 2011 to 2017 (Figure 2), as well as the relationship between annual streamflow in the two catchments from 2011 to 2017. This excludes 2016 (the wettest year), which had a much larger streamflow than the other years (Figure 2 inset).

3.1.5 | Evapotranspiration in the pasture

Evapotranspiration was measured in the pasture catchment between 2015 and 2019 using the eddy covariance method. An integrated sonic anemometer/closed-path infrared gas analyser (model CPEC200, Campbell Scientific Instruments, USA) was used in 2015; this system was replaced by an integrated sonic anemometer/open-path infrared gas analyser (IRGASON, Campbell Scientific Instruments, USA), which was used from 2016 to 2019. Turbulent flux measurements provided by these systems were collected at 10 Hz and accumulated to 30 min intervals using the software EddyPro® version 7.0.6 (LI-COR Environmental, USA), performing standard corrections to account for the detection of spikes and high frequency filtering, distance and lag between anemometer and gas analyser, density fluctuations (WPL correction), and frequency response correction. Daily evapotranspiration was calculated from the 30-min data. Gaps in the daily series up to 3 days were linearly interpolated, gaps up to 7 days were filled with the daily average of the current month, and longer gaps had the entire month substituted with the monthly average from other years. The longer gaps were 14 months in total out of the 60 months of measurements.

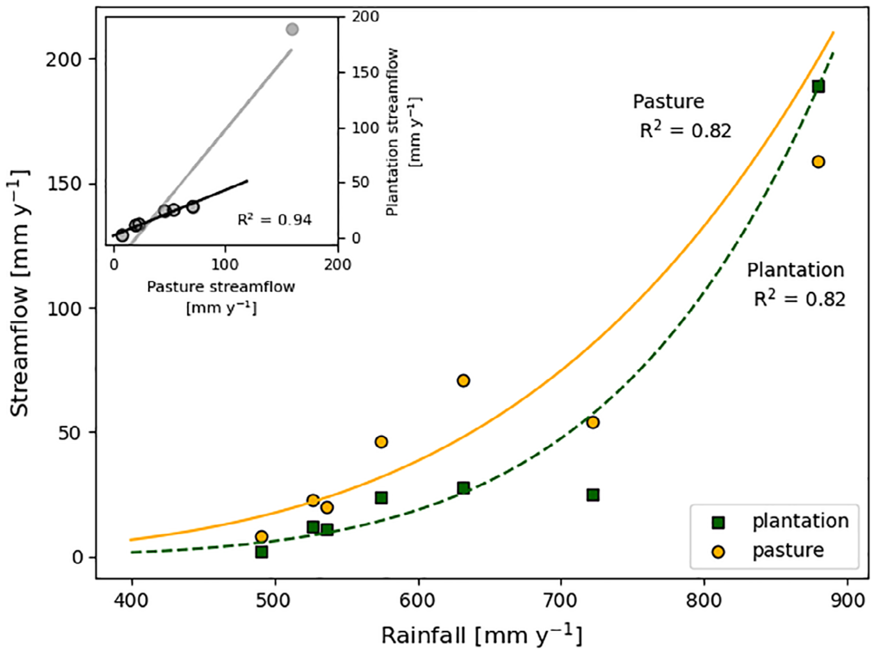

FIGURE 2 Relationship between annual rainfall and streamflow in the pasture (yellow circles) and plantation (green squares) catchments from 2011 to 2017. Inset: Linear relationship between annual streamflow in the pasture and plantation from 2011 to 2017 (grey line) and excluding the year 2016 (black line)

The evapotranspiration measurements are compared to Penman-Monteith method to estimate potential evapotranspiration, specifically the variation adopted by the Food and Agriculture Organization of the United Nations (FAO) that describes the crop reference evapotranspiration (Allen et al., 1998) based on meteorological and aerodynamic variables. The reference evapotranspiration (ET_o, mm day^{-1}) is obtained as

$$ET_o = \frac{0.408\Delta(R_n - G) + \gamma \frac{900}{T+273} u_2 (e_s - e_a)}{\Delta + \gamma(1 + 0.34\, u^2)}, \quad (1)$$

where R_n is the net radiation (MJ m^{-2} day^{-1}), G is the soil heat flux density (MJ m^{-2} day^{-1}), T is the mean daily air temperature (°C), u_2 is the wind speed at a 2 m height above the ground (m s^{-1}), e_s is the saturation vapour pressure (kPa), e_a is the actual vapour pressure (kPa), Δ is the slope of vapour pressure versus temperature curve at temperature T (kPa °C^{-1}), and γ is the psychrometric constant (kPa °C^{-1}).

3.1.6 | Tree transpiration

Tree transpiration (mm day^{-1}) was estimated using sap flow sensors (SFM 1, ICT International, Australia) in combination with dendrometer increment sensors (DBL60, ICT International) in two different locations during two different years. Both sensors were installed in seven trees from May-2017 to May-2018 in an area between the mid and upper slope of the catchment where the water table was likely deeper than 10 m from the surface. Eight trees were monitored from Feb-2019 to Feb-2020 closer to the weir in the valley of the catchment, where the water table was within 5 m of the surface.

The sap flow sensors recorded sap velocity at breast height (about 1.3 m from the ground) every 30 min using the heat ratio method. The measurements were corrected for wounding effects (0.17 mm wound width) and converted to sap flux density (SFD, cm^3 cm^{-2} h^{-1}) by accounting for sap and wood densities, specific heat capacities, and sapwood water content (Burgess et al., 2001; Marshall, 1958). An average wood density of 563.78 kg m^{-3} and water content of 38% were determined in two wood cores extracted from each of 10 trees in 2017 with increment borers (Haglöf Sweden, Sweden). These 20 cores were collected near the trees equipped with sap flow sensors.

Tree coring was also used to determine a relationship between sapwood area (A_{sw}) and tree diameter at breast height (DBH) measured by the dendrometers; A_{sw} was calculated after measuring the thickness of bark, sapwood and heartwood in 12 trees, by coring each tree once. The 12 trees were different from those used for sapflow measurements, but within the same area in the plantation. The DBH of the trees cored ranged from 13 to 33 cm, which is representative of the range of diameters within the plantation. Sapwood and heartwood were visually distinguished, using Methyl Orange as dye indicator. The relationship between A_{sw} and DBH could be obtained as: $A_{sw} = 2.16\ \mathrm{DBH}^{1.52}$ ($R^2 = 0.96$). From the relationship between A_{sw} and DBH, the change in A_{sw} over time was considered to determine tree transpiration.

3.1.7 | Evapotranspiration in the plantation

Evapotranspiration rates at the catchment scale in the plantation were calculated by up-scaling the tree transpiration rates to the planted area; direct evaporation from the planted area of the catchment was estimated from the literature (Benyon & Doody, 2015) and evapotranspiration from the unplanted areas was estimated from the measured evapotranspiration rates in the pasture.

Tree diameters were measured in 2018 (29 trees) and 2020 (156 trees) near the end of the sap flow sampling periods to develop a tree diameter distribution. Three DBH classes were defined for both periods: (I) up to 20 cm, which is about the average between all trees measured, (II) between 20 and 25 cm, and (III) larger than 25 cm. Once the percentage of trees in each class was defined, tree stand transpiration (T_{stand}, mm day^{-1}) was upscaled from the SFD of individual trees similar to Lundblad and Lindroth (2002) and Marchionni et al. (2019):

$$T_{stand} = \sum_{k=1}^{3} DBH_k \frac{N_{trees}}{A} \left(\sum_{i=1}^{n_k} \frac{(SFD \cdot A_{sw})_i}{n_k} \right), \tag{2}$$

where DBH_k is the percentage of trees in each of the 3 classes, N_{trees}/A is the number of trees per ground area, equal to 730 trees ha^{-1}, and n_k is the number of trees with sap flow sensors within a DBH class.

Evaporation rates in the planted areas of the catchment, E, are associated with soil and litter evaporation, and evaporation from rainfall intercepted by the tree canopy. This is estimated at about 48% (±7.3) of the annual rainfall in *E. globulus* plantation in the same region (Benyon & Doody, 2015). As mentioned, evapotranspiration rates from the non-planted part of the catchment, ET_{np}, were assumed to be the same as the evapotranspiration rates measured in the adjacent pasture in the same period.

Because the plantation covers 68% of the area of the catchment, the estimated annual evapotranspiration from the plantation, ET_p, in 2017, 2018 and 2019 were calculated as

$$ET_p = 0.68\,(T_{stand} + E) + 0.32\,ET_{np}. \tag{3}$$

The ET_p for 2017 and 2018 were calculated using the same T_{stand} but different contributions from E and ET_{np}. This is because T_{stand} is based on measurements from May/2017 to May/2018, while E and ET_{np} can be specified for each year. For the period 2019–2020, the sap flow measurements were from Feb/2019 to Feb/2020; thus, ET_p was calculated for only 2019 with a T_{stand} based on measurements from 2019 and filled with Jan/2020.

3.1.8 | Annual water balance

The rainfall, streamflow and head data were used to estimate catchment scale annual evapotranspiration rates following Dresel et al. (2018) and Adelana et al. (2015). Assuming no inflow to the catchments, the catchment annual water balance can be written as:

$$ET_{wb} = R - Q_s - Q_{out} - \Delta GW, \tag{4}$$

where ET_{wb} is evapotranspiration, R is rainfall, Q_s is streamflow, Q_{out} is groundwater outflow, and ΔGW is the change in groundwater storage.

The term Q_{out} in Equation (4) is calculated from the Darcy's law for one-dimensional flow using the product of the groundwater head gradient between the two furthest bores with the longest available series (bores 3019 and 64 in the pasture, and 3667 and 3668 in the plantation: Figure 1), the cross-sectional area of flow (22 584 and 27 540 m^2 for pasture and plantation, respectively, as in Adelana et al., 2015), and the hydraulic conductivity. Rising head tests estimated hydraulic conductivities of between 0.06 and 0.31 m day^{-1} in the pasture and between 0.002 and 0.18 m day^{-1} in the plantation (Barua et al., 2021).

ΔGW was estimated using the difference in hydraulic head at the beginning of January in consecutive years for each bore in both catchments. The average difference among all the bores of each catchment was then multiplied by a range of specific yield of 3%–5% (Adelana et al., 2015; Dahlhaus et al., 2002) and converted to mm for easier comparison to rainfall.

The water balance results are reported as a range of values due to the interval of values used for Q_{out}, ΔGW, and, only in the plantation, Q_s in 2018 and 2019; this is reflected into the estimated values of ET_{wb}.

4 | RESULTS

4.1 | Soil moisture and groundwater

Figure 3 shows the timeseries of climatic variables and soil moisture at several depths in both catchments. The soil water content in the pasture followed a seasonal cycle as rainfall; this cycle is still evident at 50 cm depth, disappearing at 150 cm. In the plantation, soil moisture presents a similar seasonal cycle near the surface, but with a range of fluctuation three times smaller. The soil water content remained on average approximately constant below about 50–60 cm with increasing moisture content with depth. Conversely, soil moisture content decreases with proximity to the trees (not shown). Moisture content in the pasture below about 50 cm was similar to the plantation below about 100 cm (Figure 3e).

Groundwater heads in the two catchments present very different trends, as observed by Dresel et al. (2018) for a shorter period of time. Seasonal cycles in hydraulic head were observed in every bore in the pasture with annual change of about 2 m (Figure 4a), whereas in the plantation only three bores present substantial seasonal variations (Figure 4b). These three bores were in open areas near the catchment outlet (bores 3656 and 3657) or near the stream (3669), while the ones with weak (about 0.5 m per year) or without seasonal cycles were within planted areas. As shown in Figure 4, from 2010 to 2020, the head levels in the pasture have been stable, while the head levels in most of the bores in the plantation catchment experienced a steady decline. The rate of decline reduced in most of the bores after the two wet years 2016 and 2017, except in two of them (3663 and 3668).

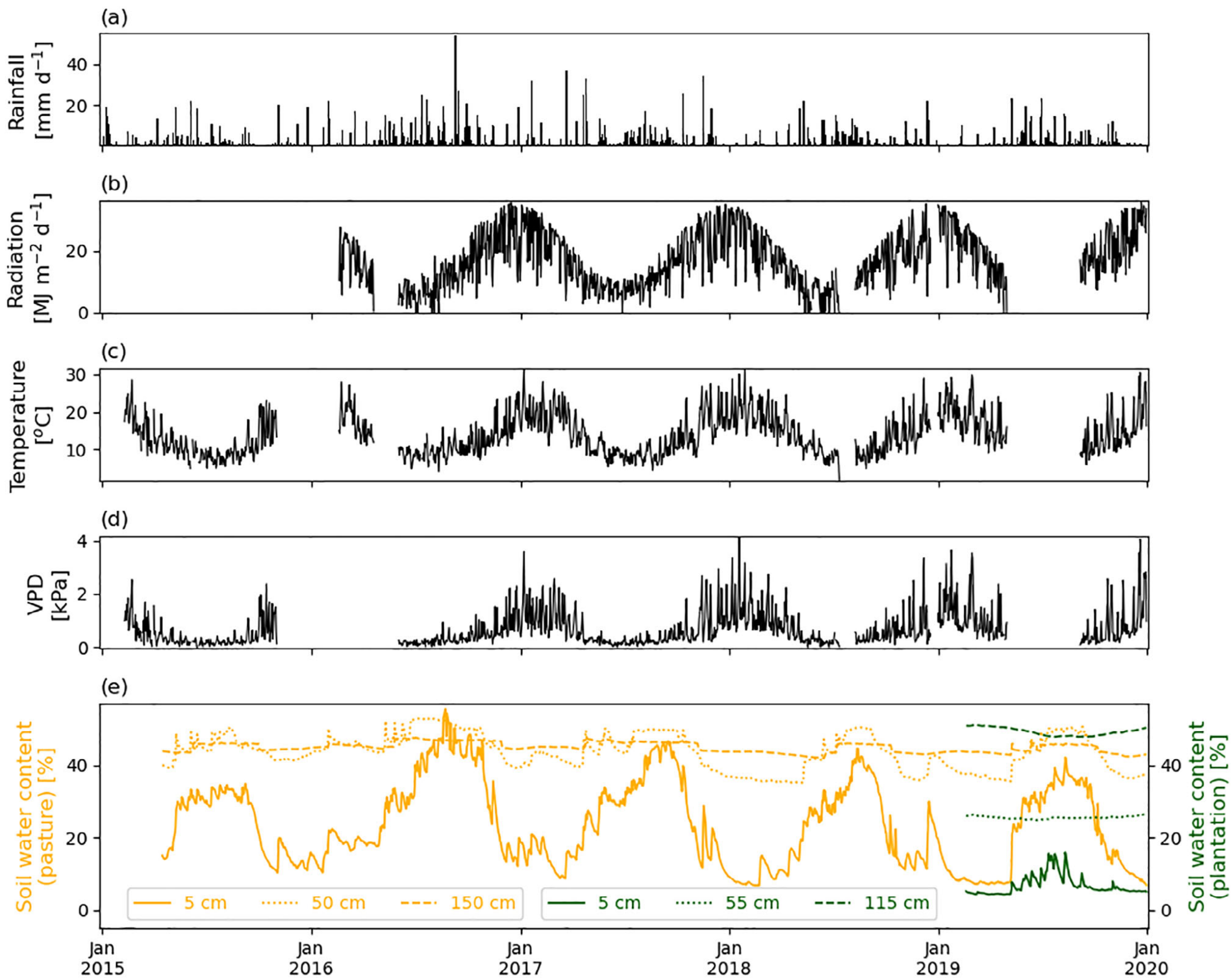

FIGURE 3 (a) Daily total rainfall (mm d^{-1}), (b) mean daily shortwave downwelling radiation (MJ m^{-2} d^{-1}), c) air temperature (°C), (d) vapour pressure deficit (VPD, kPa) and (e) mean daily soil water content (%) in the pasture (yellow longer series) and plantation (shorter green) at different soil depths

4.2 | Evapotranspiration and transpiration rates

Figure 5 shows the time series of the estimated reference crop evapotranspiration, the measured evapotranspiration from the pasture and the 2 years of up-scaled tree transpiration in two different locations in the plantation. The pasture has a very strong seasonal cycle mirroring the cycle of the grass covering the area. Grasses commence their growth in April–May and grow in winter (June–August), covering the catchment during spring. In December the grass usually starts to brown and become dormant, leaving a cover of dry grass during summer and the beginning of autumn (January to March), while reference evapotranspiration is highest. This is reflected in the evapotranspiration rates (Figure 5), with rates lower than 1 mm d^{-1} associated with soil evaporation during the dormant period and higher rates (between 3 and 4 mm d^{-1}) in spring (Sep–Nov). Before peaking at the end of spring, the pasture evapotranspiration tends to have similar rates to reference evapotranspiration.

The trees in the plantation showed very different transpiration patterns compared to the pasture. The estimated transpiration rates from the sap fluxes in the period 2017–2018, from trees in the mid- to high-slope within the catchment, showed a seasonal cycle, with peak transpiration rates between 2 and 3 mm d^{-1} (Figure 5). Conversely, the transpiration rates in the period 2019–2020, from trees in the valley near the outlet of the catchment, remained consistently at about 1 mm d^{-1} during the whole period of measurements.

The tree transpiration rates in 2019–2020 did not show any relationship to the soil water content (not shown). Focusing on the months when evapotranspiration in the pasture is associated with vegetation (Sep–Dec), different patterns can be seen in the relationship between evapotranspiration rates and soil moisture near the surface (Figure 6). The soil is usually wet within the root zone (top 30 cm) in September after the rainfall in the previous months, and the highest evapotranspiration rates tend to be around 2 mm d^{-1}. As the season progresses into spring, the solar radiation increases and the

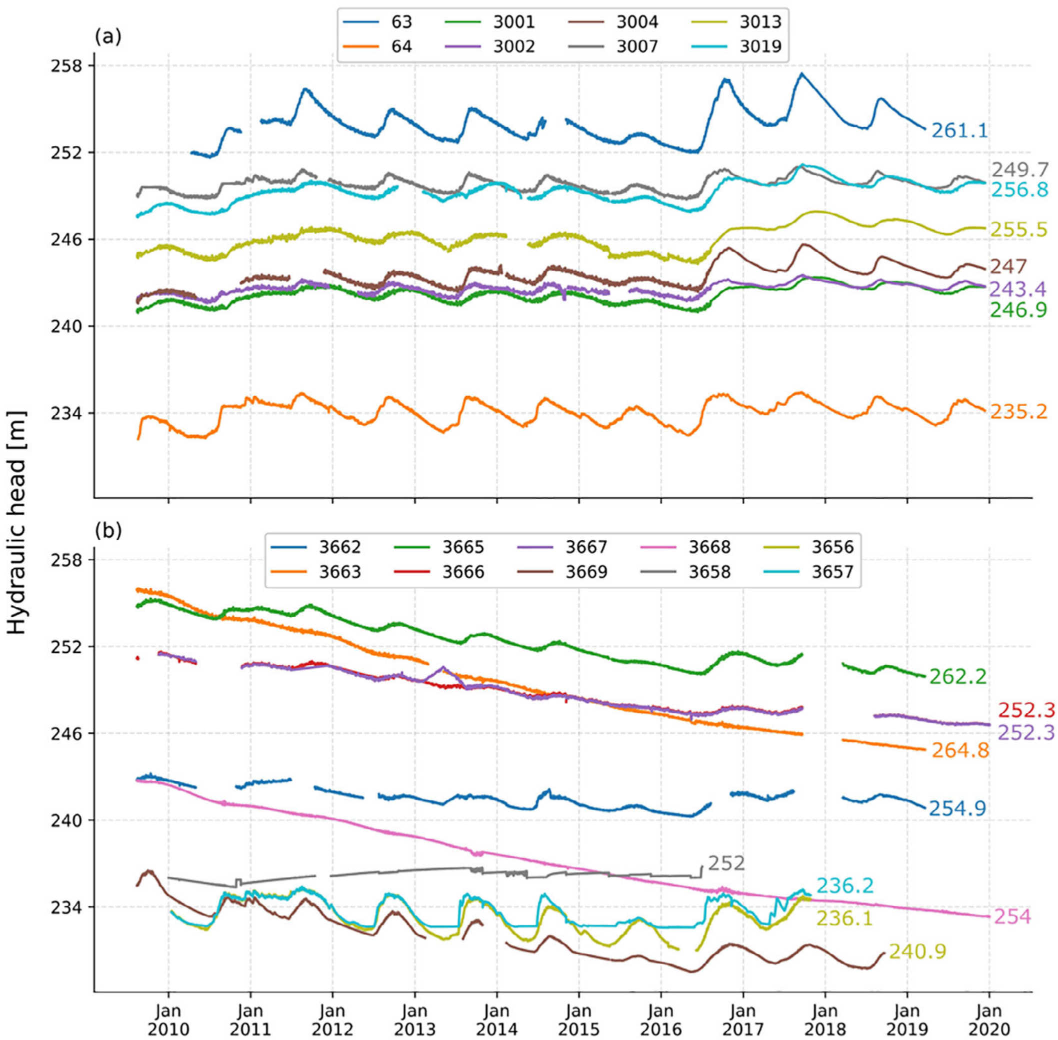

FIGURE 4 Hydraulic head measured in the pasture (a) and in the plantation (b) catchments. Numbers at the end of each head measurements are the landscape height of each bore

soil is still wet even though rainfall events start reducing. In October and November, the pasture generally experiences the largest evapotranspiration rates (above 3 mm d^{-1}) being neither water nor energy limited. In late November and December, the soil moisture levels generally drop below 25% and evapotranspiration rates drop (Figure 6) as the vegetation browns and becomes dormant in late December. Some sporadic rainfall events in December might trigger some short periods of higher evapotranspiration, as shown for example in 2018 (Figure 6c).

The patterns in Figure 6 suggest that the vegetation in the pasture transitions from energy limited conditions in late winter and early spring to water limited conditions in late spring and early summer. This is also shown in Figure 7, where evapotranspiration from the pasture is related to solar radiation and VPD. In the period between September and November, evapotranspiration rates tend to increase from 1–2 to 3–5 mm day^{-1} as radiation and VPD increase, being lower in September because of the lower radiation and VPD values (maximum at 15 MJ m^{-2} day^{-1} and 1 kPa, respectively). In December, because of the much-reduced water availability, the evapotranspiration declines as radiation and VPD increase. There is a statistically significant linear relationship ($p < 0.001$) between daily evapotranspiration and climatic variables (radiation and VPD) in the pasture for every September measured and this relationship tends to weaken as the season progress to summer (Figure 7a–c, e–g). At the end of spring (Nov), the relationship seems to differ in magnitude between wet and dry years (Figure 7c, g). During the wetter years of 2016 (879 mm y^{-1}) and 2017 (681 mm y^{-1}) the relationship between daily evapotranspiration rates and climatic variables is twice as high as in the following years that experienced a decrease in rainfall by about 30%–50% (2018 and 2019, 522 mm y^{-1} and 464 mm y^{-1}, respectively). In December, this relationship appears to reverse for solar radiation (Figure 7d) and evapotranspiration in the pasture decreases non-linearly with VPD (Figure 7h).

The relationship with radiation and VPD is not as evident for the tree transpiration in the plantation (Figure 8). As transpiration had distinct magnitude in each location measured, these were separated in

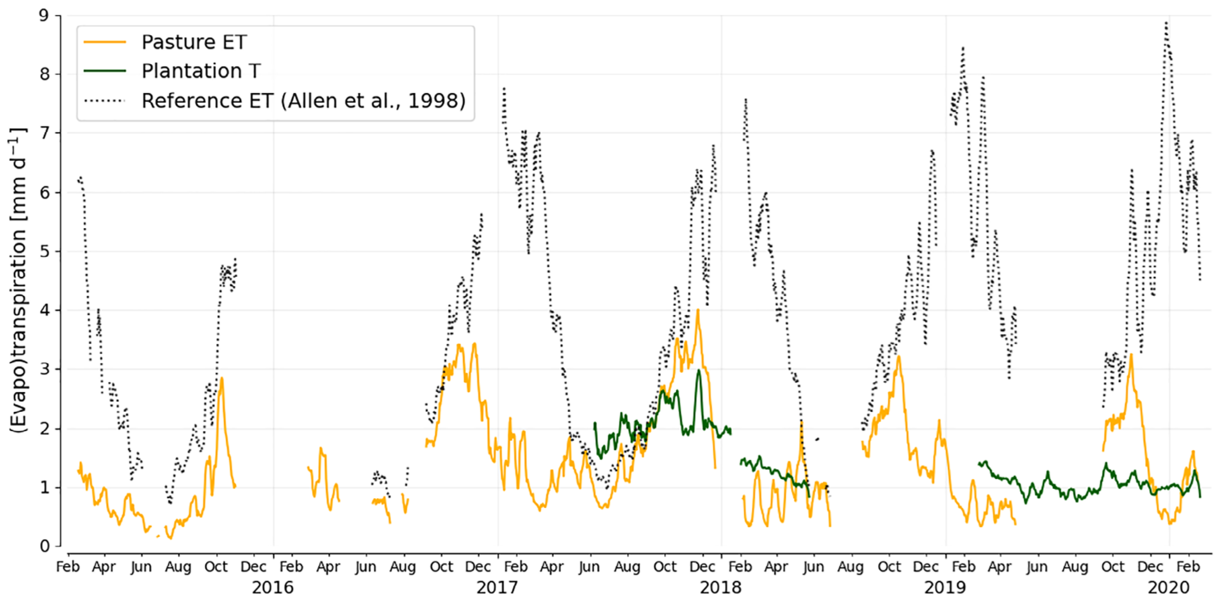

FIGURE 5 10-day moving averages of pasture daily evapotranspiration (ET, mm d^{-1}), plantation daily transpiration (T, mm d^{-1}) and estimated daily reference ET (mm d^{-1}) using field measurements at the pasture

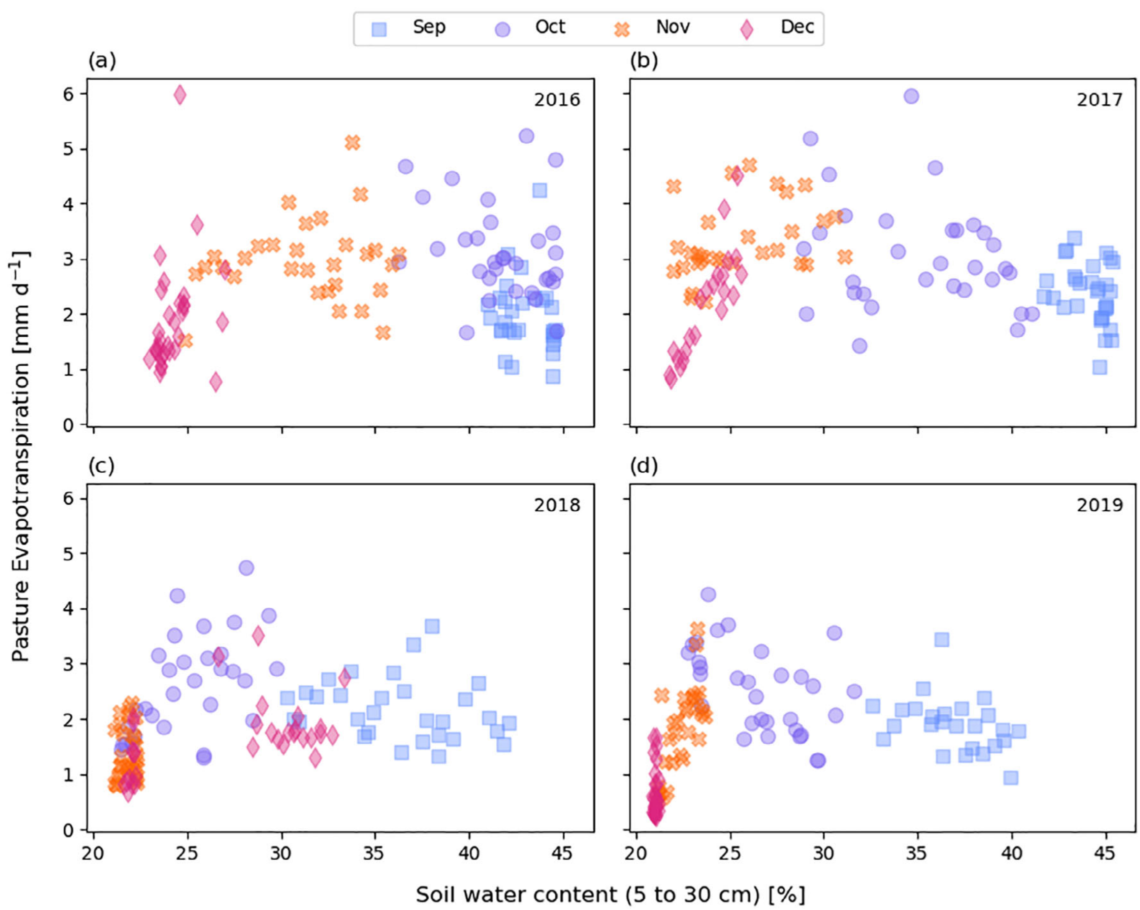

FIGURE 6 Relationship between pasture evapotranspiration (mm d^{-1}) and average soil water content (%) in the top 30 cm of soil for the months of September (square), October (circle), November (x) and December (diamond). Each panel represents a different year from 2016 (a) to 2019 (d)

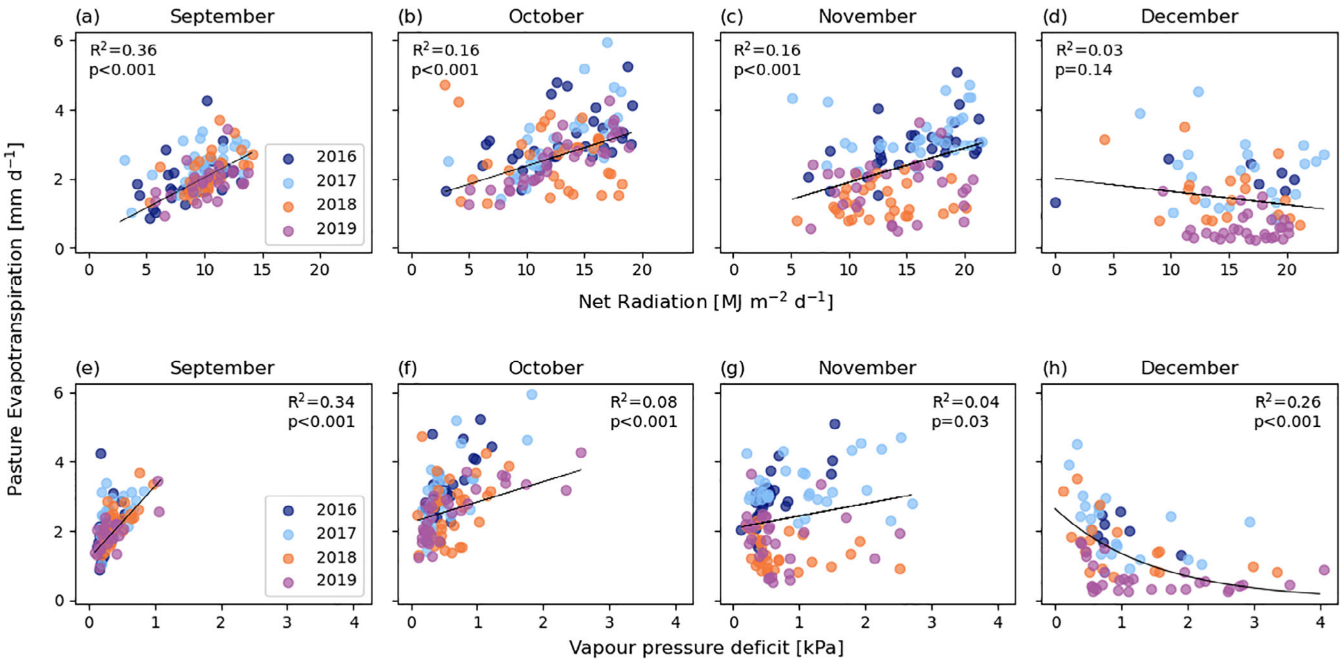

FIGURE 7 Relationship of daily pasture evapotranspiration (mm d^{-1}) with (a–d) average daily net radiation (MJ m^{-2} d^{-1}) and (e–h) vapour pressure deficit (kPa)

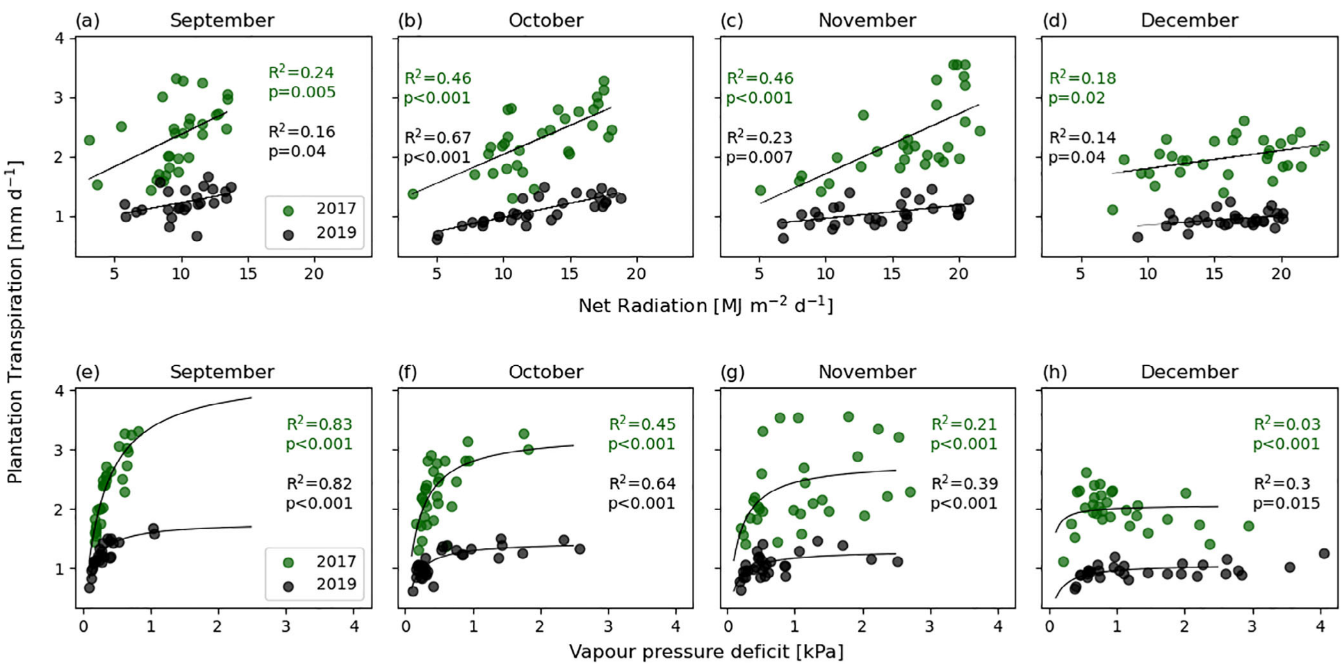

FIGURE 8 Relationship between daily plantation transpiration (mm d^{-1}) and in the four panels on the top (a–d): Average daily radiation (MJ m^{-2} d^{-1}) and bottom (e–h): Vapour pressure deficit (kPa)

the analysis, but still had similar statistical significance (Figure 8). Similar to the pasture, the plantation transpiration increases as radiation increases, with October showing the strongest relationship, when daily radiation reaches highs above 15 MJ m^{-2} d^{-1} (Figure 8b). In relation to VPD, the tree transpiration appears to consistently follow an exponential function (Whitley et al., 2013) with lower rates as summer approaches. As expected, transpiration rates reach a plateau as the VPD increases.

The changes between spring and summer in both catchments are also observed at a diurnal level with high pasture evapotranspiration, which surpasses plantation transpiration during spring (Figure 9c) and declines to only soil evaporation during summer as the grass enters

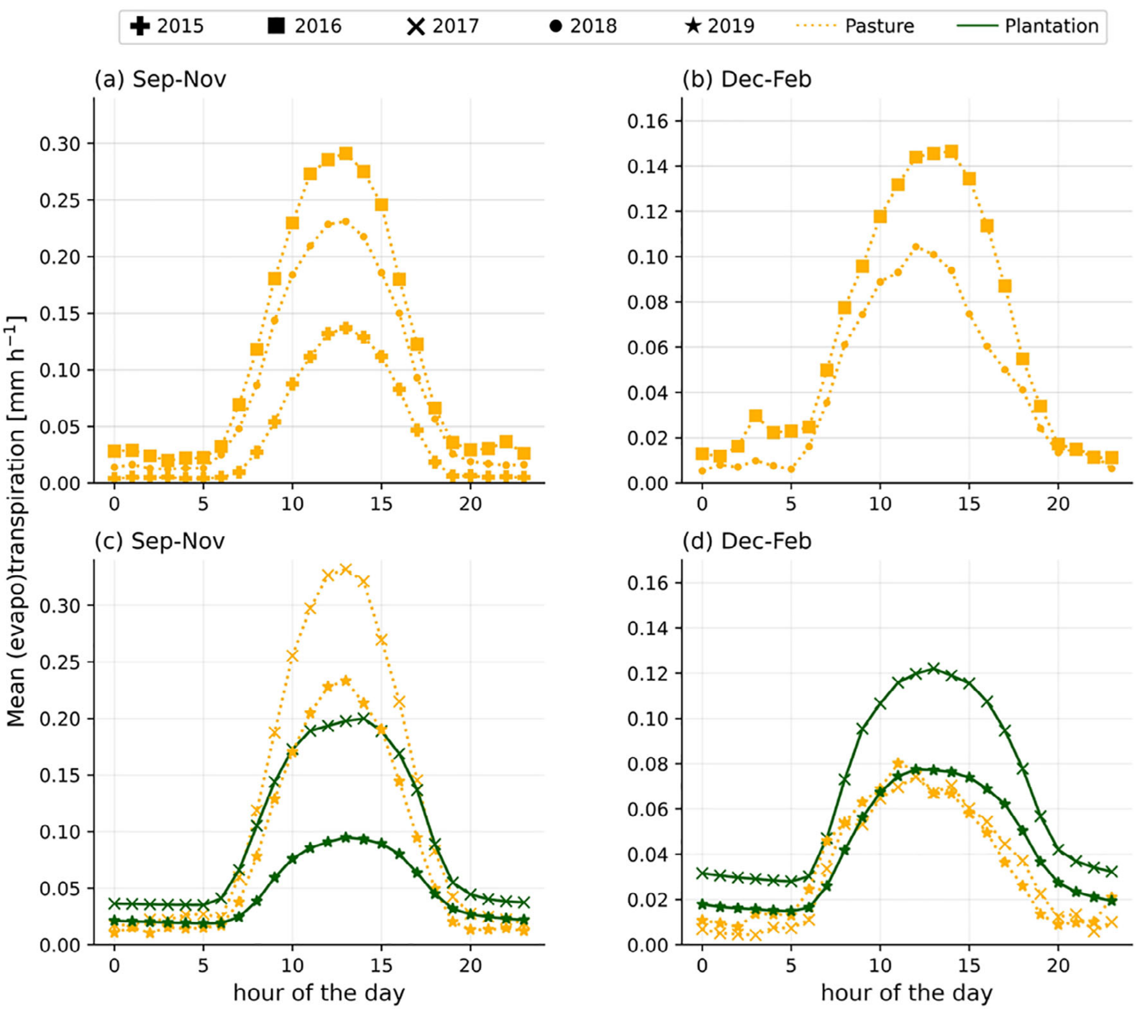

FIGURE 9 Diurnal course (hourly means) of evapotranspiration (mm h^{-1}) in pasture catchment and transpiration in the plantation catchment, across two different seasons: Spring (Sep–Nov; panels a and c) and summer (Dec–Feb; panels b and d). Note that the scale is different between seasons. (a) and (b) refer to the mean of 2015, 2016, and 2018, while (c) and (d) to the mean of 2017 and 2019

dormancy. By the end of summer, pasture evapotranspiration decreases about 80% while the plantation transpiration decreases about 50% from peaks in spring. The pasture had well-defined peaks of evapotranspiration rates during the day, at about 1 pm (Figure 9b, d), while trees in the plantation sustained high transpiration rates for longer in the middle of the day, regardless of the season (Figure 9c, d).

4.3 | Water balance

The estimated annual values of the components of the water balance are reported in Table 1. The evapotranspiration rates in the plantation catchment estimated using Equation (4) (ET_{wb}) exceeded the rates in the pasture by about 30 mm a year on average. In the plantation catchment, ET_{wb} often exceeded annual rainfall especially when annual rainfall was below about 500 mm a year (i.e., in 2015, 2018, and 2019); this happened only in 2015 (driest year) in the pasture catchment.

The estimates of evapotranspiration are comparable to field measurements in both catchments. The mean absolute difference between ET_{wb} and the evapotranspiration rates from measurements is about 98 mm in the pasture (eddy covariance measurements, ET_{ec}), with the largest difference in 2015, and 31 mm in the plantation (ET_p). Over the 5 years of measurements, ET_{wb} was on average 88% of the rainfall in the pasture and 93% in the plantation, varying from a minimum of 74% and 75% of rainfall in the wettest year to 102% and 103% in a dry year, respectively.

In relation to the other components of the water balance, streamflow (Q_s) and change in groundwater storage (ΔGW) appear to be directly connected to the annual rainfall in both catchments. Streamflow is normally higher in the pasture than it is in the plantation but overall accounts for less than 10% of the rainfall, with exception of 2016 when it represented about 20% of the rainfall (Table 1). Changes in groundwater storage were different between catchments. The storage in the pasture declined in dry years but recovered considerably in wet years; the storage in the plantation consistently declined apart

TABLE 1 Components of the annual water balance (mm y^{-1}) from 2015 to 2019, including groundwater (*GW*) and measurement estimates of evapotranspiration (*ET*) for the pasture (ET_{ec}) and plantation (ET_p) catchments

	2015	2016	2017	2018	2019	Average
Pasture						
Rainfall	491	879	681	522	464	607
Streamflow	8 (2)	159 (18)	43 (7)	44 (9)	30 (6)	57 (9)
Δ*GW* storage	−30 (−6) ± 7	60 (7) ± 15	15 (2) ± 4	−20 (−4) ± 5	−5 (−1) ± 1	4 (1)
GW outflow	11 (2) ± 7	11 (1) ± 7	12 (2) ± 8	12 (2) ± 8	11 (4) ± 7	11 (2)
ET_{wb}	502 (102) ± 14	649 (74) ± 22	611 (90) ± 12	486 (93) ± 13	428 (92) ± 8	535 (88)
ET_{ec}	325 (66)	491 (56)	537 (79)	416 (80)	415 (89)	437 (72)
Plantation						
Rainfall	491	879	681	522	464	607
Streamflow	2 (0.4)	189 (21)	27 (4)	16 (3) ± 9	8(2) ± 3	48 (8)
Δ*GW* storage	−25 (−5) ± 6	20 (2) ± 5	−5 (−1) ± 1	−32 (−6) ± 8	−20 (−4) ± 5	−12 (−2)
GW outflow	7 (1) ± 7	7 (1) ± 7	6 (1) ± 6	6 (1) ± 6	8 (2) ± 8	7 (1)
ET_{wb}	507 (103) ± 13	663 (75) ± 12	653 (96) ± 7	532 (102) ± 23	468 (101) ± 16	565 (93)
ET_p			597 (88)[a]	506 (97)[a]	480 (103)[b]	

Note: ET_{wb} is estimated from Equation (4). In brackets, the percentage of rainfall for each component. ET_p in the plantation was calculated using sap flow measurements across 2017–2018[a] and 2019–2020[b].

from 2016 (Figure 4) which was a year of unusually high annual rainfall (879 mm).

5 | DISCUSSION

5.1 | Evapotranspiration and transpiration rates

The measured evapotranspiration rates in the pasture and the estimated transpiration rates in the plantation using sap flow data show very different patterns and relationships with atmospheric variables. The evapotranspiration rates between September and December when the pasture releases most water to the atmosphere appeared to be limited by different environmental variables (Figures 6 and 7). In September and part of October, the pasture has access to water stored in the soil following the winter rains, but the lower solar radiation and temperature limit the evapotranspiration rates, as confirmed by the low reference evapotranspiration (Figure 5). In late October and November, radiation and VPD lead to the highest rates of evapotranspiration in the pasture. In late November and in December, the combination of low soil water content near the surface, where most of the roots are expected to be, and high solar radiation and air temperature causes a fall in evapotranspiration rates. The pasture thus switched from an energy-limited to a water-limited system over the course of a few months. There are not many studies analysing this behaviour in Australian pastures and grasslands. In southwest Australia, Ward and Dunin (2001) showed that actual evapotranspiration in winter was very similar to potential evapotranspiration, which is driven by meteorological variables such as solar radiation. In spring, however, actual evapotranspiration was reduced because of water limitation.

Tree transpiration was very different in the two locations and comparable to that measured by Dean et al. (2016) in a catchment in western Victoria; Dean et al. (2016) sampled trees at different elevations where the depths to the water table were different. Trees in areas with very shallow water tables had smaller transpiration rates. *E. globulus* are known for an intermediate salt-waterlogging tolerance (Blake & Reid, 1981; Meddings et al., 2001; Sena Gomes & Kozlowski, 1980), thus the decreased transpiration rates might be attributed to a high groundwater salinity, which is a relevant issue in the region (Adelana et al., 2015; Dahlhaus et al., 2000; Dean et al., 2016). In addition, tree transpiration may be intensified after the 20 mm rainfall threshold is exceeded, as found by Zeppel et al. (2008) in a woodland in southeast Australia. In our study, intense rainfall pulses well above this threshold occurred at the end of 2017 (Figure 3a), while the 2019–2020 period lacked similar strong rainfall pulses.

Water-use and evapotranspiration are directly linked to radiation, forming a bell shape diel-cycle (Figure 9). Tree transpiration tends to have more constant rates in the middle of the day (flat top) than pasture evapotranspiration (Crosbie et al., 2007). However, in tree belts measured by Crosbie et al. (2007), they reported a steep increase/decrease in the beginning/end of the day compared to the pasture. Conversely, our results show a smooth increase/decrease, similar to the pasture (Figure 9c, d). Differently from Crosbie et al. (2007), who reported only 1 day of measurements, we presented averages by season, which might have smoothed out the results; additionally, the edge effect is more significant in tree belts, where trees are more susceptible to the incidence of solar radiation, while in the plantation there is more competition for solar energy (Ellis et al., 2005).

Daily tree transpiration rates appeared to increase with radiation, as expected (Macinnis-ng et al., 2016; Zeppel et al., 2004) (Figure 8 a-d); daily tree transpiration also increased with VPD when this was lower than about 1 kPa and tended to reach a plateau for larger values of VPD (Figure 8e–h), as shown in other studies on *E. globulus* (David et al., 1997; O'Grady et al., 2008). Different from the pasture, *E. globulus* trees have the ability to regulate stomatal aperture and reduce water losses when the VPD increases (Macfarlane et al., 2004; Pereira et al., 1987).

5.2 | Water balance

The evapotranspiration rates estimated from the water balance and from diverse measurements were similar. The water balance in the pasture was higher than eddy covariance measurements (ET_{ec}), especially in 2015. In the pasture, it was assumed that ET_{ec} corresponded to the catchment evapotranspiration; however, only a portion of the catchment was included in the footprint of the eddy covariance measurements, corresponding to the mid-slope. In very dry years, such as 2015, the lowest part of the catchment, near the drainage line and the creek, may generate higher evapotranspiration rates as the soil remains wetter. This might explain the lower values of ET_{ec} in relation to ET_{wb}. Additionally, substantially lower annual ET in 2015 may be due to long gaps of data at the beginning and end of the year, totalling to about 3 months of missing data.

Studies often report a possible underestimation of transpiration estimates from sap flow measurements (Ford et al., 2007; Schlesinger & Jasechko, 2014; Steppe et al., 2010; Vandegehuchte & Steppe, 2013). However, after accounting for interception and litter evaporation, estimates of evapotranspiration in the plantation (ET_p) were consistent with water balance estimates (ET_{wb}), with the largest difference in 2017 when ET_{wb} is only 7% of the annual rainfall higher than ET_p.

Dresel et al. (2018) found annual evapotranspiration to be on average 87% of annual precipitation in the pasture and 102% in the plantation, in the period 2011–2016. Although these values are comparable to both our water balance and measurements, the estimated ET_{wb} in 2015 and 2016 presented here differ from those reported in Dresel et al. (2018). The differences mainly stem from the calculation of the changes in groundwater storage, ΔGW, which was calculated here using the average change in groundwater levels from all the bores, while Dresel et al. (2018) allocated each bore to a portion of the catchment area and calculated the change in storage using a weighted average based on these areas. The values of ET_{wb} calculated in the present study are lower than those in Dresel et al. (2018) in 2015 and larger in 2016. The estimated ET_{wb} in the pasture in 2015 and 2016 are closer to ET_{ec} than the estimates by Dresel et al. (2018).

Transpiration in plantations seems to be as important as interception and litter evaporation (Silva et al., 2022). Benyon and Doody (2015) found that the interception and litter evaporation from the forest floor of *E. globulus* plantations, in the same region as the present study, was on average 19% and 29% of annual rainfall, respectively. Therefore, tree transpiration and about 48% of interception and evaporation in years with rainfall lower than about 500 mm make evapotranspiration in the plantation larger than total rainfall. This imbalance between annual rainfall and evapotranspiration is reflected on groundwater heads, which declined over time (Figure 4b). The groundwater heads in the plantation do not show strong seasonal fluctuations, likely because the transpiration rates are sustained throughout the year and interception and litter evaporation are also occurring throughout the year, as the trees are evergreen. These patterns suggest that the plantation is limiting groundwater recharge by reducing the amount of water infiltrating the soil (i.e., interception and litter evaporation) and taking up water from the unsaturated zone for transpiration, without necessarily transpiring water from the saturated zone as hinted in other studies from the same site (Dresel et al., 2018) or observed in other locations (Benyon et al., 2006).

The pasture presents very different patterns. The groundwater levels remained approximately stable over the period 2009–2019 (Figure 4a); evapotranspiration rates were estimated to be lower than annual rainfall in most years (Table 1), as also reported by Dresel et al. (2018). Additionally, there are strong seasonal cycles in groundwater levels in the pasture, with increases during autumn and winter, when most rainfall occurs, and drops during spring and summer.

Accounting for only about 8%–9% of rainfall in both catchments, the streamflow is higher in the pasture compared to the plantation, except for 2016 (Table 1). In 2016, streamflow was possibly overestimated because the region received intense rainfall that often carried debris to the weir, which caused slower drainage and, thus, higher levels were recorded. The streamflow is highly dependent on rainfall (Adelana et al., 2015; Dresel et al., 2018) and, in the plantation catchment, is mostly generated through the riparian zone. Therefore, the lower streamflow in the plantation compared to the pasture might not be related to land-use, but likely associated with the geomorphology of the two catchments and the distinct hydraulic conductivities, despite the proximity of the catchments (Barua et al., 2021).

The water balance calculations in Table 1 show that the difference in evapotranspiration rates between the pasture and plantation catchments, which are on average $\sim$5% for the period under analysis, are enough to cause a reduction in the groundwater storage in the plantation since 2011 (Dresel et al., 2018). Jackson et al. (2009) mentioned that as annual precipitation reaches values below 800 mm, differences in evapotranspiration between grassed and treed systems are likely to disappear. Our findings suggest that annual evapotranspiration losses exceed annual rainfall when the annual rainfall is lower than about 500 mm. Establishing plantations that promote large interception and litter evaporation might thus cause a tipping point in the water balance inducing a gradual reduction in groundwater resources.

6 | CONCLUSION

This study aimed at identifying and quantifying the differences in the evapotranspiration rates in two headwater catchments with very distinct land uses (a pasture and a plantation) and understand how these differences affected the water balance of the two catchments. With increased pressure on water resources through agriculture activities and changing climate, it is urgent to know evapotranspiration patterns across different rural land-uses to provide support for appropriate management practices.

The evapotranspiration rates experienced very different patterns during the year. Evapotranspiration in the pasture showed a marked seasonal cycle, with large evapotranspiration rates in spring and early summer, and very low rates in summer. Conversely, the trees in the plantation transpired water more uniformly during the year; because the trees were evergreen, it is expected that interception and litter evaporation would also occur throughout the year. Although the pasture showed evapotranspiration rates that were larger than tree transpiration in spring, the annual evapotranspiration in the pasture was estimated to be lower than the plantation, where the measured contribution of tree transpiration to the annual evapotranspiration fluxes was estimated to be similar to the interception and litter evaporation, which was calculated as a percentage of annual rainfall following observations from other studies. These differences were comparable to the values estimated from water balance calculations obtained from measurements of precipitation, streamflow, and groundwater levels. Overall, the annual evapotranspiration in the pasture remained lower or close to the annual precipitation, while in the plantation the annual evapotranspiration was larger than precipitation in the driest years.

The different evapotranspiration rates were reflected in the water table levels in the two catchments. In the past decade, the groundwater levels in the pasture remained fairly stable with strong seasonal cycles visible across the whole catchment. In the plantation, the groundwater levels decreased over time, with seasonal cycles visible only in bores installed in non-planted areas. The trees in the plantation seem to reduce the groundwater recharge, with no evidence of direct uptake from groundwater.

Although the annual evapotranspiration rates in the two catchments were not largely different, the evapotranspiration rates in the plantation appeared to be larger than rainfall when annual rainfall was lower than about 500 mm; this is likely the cause of dropping groundwater levels. Plantations in arid and semiarid areas, might thus cause a tipping point in the water balance affecting the water storage of small upland catchments.

ACKNOWLEDGEMENTS

We thank Rob Lawrance and Georgie Luckock for allowing us to access their farm and PF-Olsen Australia for the access to the plantation. The research was supported by the Australian Research Council (grants no. LP140100871 and DP180101229). Open access publishing facilitated by Monash University, as part of the Wiley - Monash University agreement via the Council of Australian University Librarians.

DATA AVAILABILITY STATEMENT

The data that support the findings of this study are available from the corresponding author upon reasonable request.

ORCID

Alberto M. L. Peixoto Neto https://orcid.org/0000-0001-5308-5931
Ian Cartwright https://orcid.org/0000-0001-5300-4716

REFERENCES

Adelana, S. M., Dresel, P. E., Hekmeijer, P., Zydor, H., Webb, J. A., Reynolds, M., & Ryan, M. (2015). A comparison of streamflow, salt and water balances in adjacent farmland and forest catchments in South-Western Victoria, Australia. *Hydrological Processes*, *29*(6), 1630–1643. https://doi.org/10.1002/hyp.10281

Allen, R. G., Pereira, L. S., Raes, D., Smith, M., & Ab, W. (1998). Crop evapotranspiration-guidelines for computing crop water requirements-FAO irrigation and drainage paper 56. *FAO, Rome*, *300*(9), D05109.

Azarnivand, A., Camporese, M., Alaghmand, S., & Daly, E. (2020). Modeling hydrological impacts of afforestation on intermittent streams. *Science of the Total Environment*, *728*, 138748. https://doi.org/10.1016/j.scitotenv.2020.138748

Barson, M. (2000). Land cover change in Australia: Results of the collaborative Bureau of Rural Sciences—state agencies' project on remote sensing of agricultural land cover change. Bureau of Rural Sciences: Kingston, A.C.T.

Barua, S., Cartwright, I., Dresel, P. E., Morgenstern, U., McDonnell, J. J., & Daly, E. (2022). Sources and mean transit times of intermittent streamflow in semi-arid headwater catchments. *Journal of Hydrology*, *604*, 127208. https://doi.org/10.1016/j.jhydrol.2021.127208

Barua, S., Cartwright, I., Evan Dresel, P., & Daly, E. (2021). Using multiple methods to investigate the effects of land-use changes on groundwater recharge in a semi-arid area. *Hydrology and Earth System Sciences*, *25*(1), 89–104. https://doi.org/10.5194/hess-25-89-2021

Beck, H. E., Zimmermann, N. E., McVicar, T. R., Vergopolan, N., Berg, A., & Wood, E. F. (2018). Present and future Köppen-Geiger climate classification maps at 1-km resolution. *Scientific Data*, *5*(1), 180214. https://doi.org/10.1038/sdata.2018.214

Benyon, R. G., & Doody, T. M. (2015). Comparison of interception, forest floor evaporation and transpiration in *Pinus radiata* and *Eucalyptus globulus* plantations. *Hydrological Processes*, *29*(6), 1173–1187. https://doi.org/10.1002/hyp.10237

Benyon, R. G., Theiveyanathan, S., & Doody, T. M. (2006). Impacts of tree plantations on groundwater in South-Eastern Australia. *Australian Journal of Botany*, *54*(2), 181–192. https://doi.org/10.1071/BT05046

Blake, T. J., & Reid, D. M. (1981). Ethylene, water relations and tolerance to waterlogging of three Eucalyptus species. *Functional Plant Biology*, *8*(6), 497–505.

Bradshaw, C. J. A. (2012). Little left to lose: Deforestation and forest degradation in Australia since European colonization. *Journal of Plant Ecology*, *5*(1), 109–120. https://doi.org/10.1093/jpe/rtr038

Brown, A. E., Podger, G. M., Davidson, A. J., Dowling, T. I., & Zhang, L. (2007). Predicting the impact of plantation forestry on water users at local and regional scales. An example for the Murrumbidgee River basin, Australia. *Forest Ecology and Management*, *251*(1–2), 82–93. https://doi.org/10.1016/j.foreco.2007.06.011

Brown, A. E., Zhang, L., McMahon, T. A., Western, A. W., & Vertessy, R. A. (2005). A review of paired catchment studies for determining changes in water yield resulting from alterations in vegetation. *Journal of Hydrology*, *310*(1–4), 28–61. https://doi.org/10.1016/j.jhydrol.2004.12.010

Brown, S. C., Versace, V. L., Lester, R. E., & Walter, M. T. (2015). Assessing the impact of drought and forestry on streamflows in South-Eastern Australia using a physically based hydrological model. *Environmental Earth Sciences*, *74*(7), 6047–6063. https://doi.org/10.1007/s12665-015-4628-8

Buck, A. L. (1981). New equations for computing vapour pressure and enhancement factor. *Journal of Applied Meteorology*, *20*(12), 1527–1532. https://doi.org/10.1175/1520-0450(1981)020<1527:nefcvp>2.0.co;2

Burgess, S. S. O., Adams, M. A., Turner, N. C., Beverly, C. R., Ong, C. K., Khan, A. A. H., & Bleby, T. M. (2001). An improved heat pulse method to measure low and reverse rates of sap flow in woody plants. *Tree Physiology*, *21*(9), 589–598. https://doi.org/10.1093/treephys/21.9.589

Cartwright, I., Weaver, T. R., Fulton, S., Nichol, C., Reid, M., & Cheng, X. (2004). Hydrogeochemical and isotopic constraints on the origins of dryland salinity, Murray Basin, Victoria, Australia. *Applied Geochemistry*, *19*(8), 1233–1254. https://doi.org/10.1016/j.apgeochem.2003.12.006

Colville, J. S., & Holmes, J. W. (1972). Water table fluctuations under forest and pasture in a karstic region of Southern Australia. *Journal of Hydrology*, *17*(1–2), 61–80. https://doi.org/10.1016/0022-1694(72)90066-2

Crosbie, R. S., Wilson, B., Hughes, J. D., & McCulloch, C. (2007). The upscaling of transpiration from individual trees to areal transpiration in tree belts. *Plant and Soil*, *297*(1), 223–232. https://doi.org/10.1007/s11104-007-9420-4

Dahlhaus, P. G., Heislers, D., & Dyson, P. (2002). Groundwater flow systems. Report No. GHCMA 02/02. Buninyong, VIC.

Dahlhaus, P. G., MacEwan, R. J., Nathan, E. L., & Morand, V. J. (2000). Salinity on the southeastern Dundas Tableland, Victoria. *Australian Journal of Earth Sciences*, *47*(1), 3–11. https://doi.org/10.1046/j.1440-0952.2000.00759.x

Daneshmand, H., Alaghmand, S., Camporese, M., Talei, A., & Daly, E. (2019). Water and salt balance modelling of intermittent catchments using a physically-based integrated model. *Journal of Hydrology*, *568*, 1017–1030. https://doi.org/10.1016/j.jhydrol.2018.11.035

David, T. S., Ferreira, M. I., David, J. S., & Pereira, J. S. (1997). Transpiration from a mature *Eucalyptus globulus* plantation in Portugal during a spring-summer period of progressively higher water deficit. *Oecologia*, *110*(2), 153–159. https://doi.org/10.1007/PL00008812

Dean, J. F., Camporese, M., Webb, J. A., Grover, S. P., Dresel, P. E., & Daly, E. (2016). Water balance complexities in ephemeral catchments with different land uses: Insights from monitoring and distributed hydrologic modeling. *Water Resources Research*, *52*(6), 4713–4729. https://doi.org/10.1002/2016WR018663

Dean, J. F., Webb, J. A., Jacobsen, G. E., Chisari, R., & Dresel, P. E. (2015). A groundwater recharge perspective on locating tree plantations within low-rainfall catchments to limit water resource losses. *Hydrology and Earth System Sciences*, *19*(2), 1107–1123. https://doi.org/10.5194/hess-19-1107-2015

Downham, R., & Gavran, M. (2020). Australian plantation statistics 2020 update. ABARES, Canberra. https://doi.org/10.25814/5ecb5411d91fa

Dregne, H. E. (2002). Land degradation in the drylands. *Arid Land Research and Management*, *16*(2), 99–132. https://doi.org/10.1080/153249802317304422

Dresel, P. E., Dean, J. F., Perveen, F., Webb, J. A., Hekmeijer, P., Adelana, S. M., & Daly, E. (2018). Effect of Eucalyptus plantations, geology, and precipitation variability on water resources in upland intermittent catchments. *Journal of Hydrology*, *564*(May), 723–739. https://doi.org/10.1016/j.jhydrol.2018.07.019

Ellis, T., Hatton, T., & Nuberg, I. (2005). An ecological optimality approach for predicting deep drainage from tree belts of alley farms in water-limited environments. *Agricultural Water Management*, *75*(2), 92–116. https://doi.org/10.1016/j.agwat.2004.12.004

Foley, J. A., DeFries, R., Asner, G. P., Barford, C., Bonan, G., Carpenter, S. R., Chapin, F. S., Coe, M. T., Daily, G. C., Gibbs, H. K., Helkowski, J. H., Holloway, T., Howard, E. A., Kucharik, C. J., Monfreda, C., Patz, J. A., Prentice, I. C., Ramankutty, N., & Snyder, P. K. (2005). Global consequences of land use. *Science*, *309*(5734), 570–574. https://doi.org/10.1126/science.1111772

Ford, C. R., Hubbard, R. M., Kloeppel, B. D., & Vose, J. M. (2007). A comparison of sap flux-based evapotranspiration estimates with catchment-scale water balance. *Agricultural and Forest Meteorology*, *145*(3–4), 176–185. https://doi.org/10.1016/j.agrformet.2007.04.010

Gribovszki, Z., Kalicz, P., Balog, K., Szabó, A., Tóth, T., Csáfordi, P., Metwaly, M., & Szalai, S. (2017). Groundwater uptake of different surface cover and its consequences in great Hungarian plain. *Ecological Processes*, *6*(1), 1–9. https://doi.org/10.1186/s13717-017-0106-4

Hatton, T. J., Ruprecht, J., & George, R. J. (2003). Preclearing hydrology of the Western Australia wheatbelt: Target for the future? *Plant and Soil*, *257*(2), 341–356. https://doi.org/10.1023/A:1027310511299

Hekmeijer, P., Zydor, H., Reid, M., Epsom, V., Iven, I., Field, M., Lawrance, R., Luckock, G., Youngman, H., & Buttas, G. (2011). Catchment scale impacts on land use change in south-west Victoria (CMI 102920). Report on 2009–10 drilling and weir construction programs. Victoria Department of Primary Industries, Epsom, VIC (Cmi 102920).

Herron, N., Davis, R., Dawes, W., & Evans, R. (2003). Modelling the impacts of strategic tree plantings on salt loads and flows in the Macquarie River catchment, NSW, Australia. *Journal of Environmental Management*, *68*(1), 37–50. https://doi.org/10.1016/S0301-4797(02)00230-X

Iglesias-Trabado, G., Arballeira-Tenreiro, R., & FolgueiraLozana, J. (2009). Eucalyptus universalis: global cultivated eucalypt forests map. Version 1.2. *Eucalyptologics Information Resources on Eucalypt Cultivation Worldwide*. https://git-forestry-blog.blogspot.com/

Jackson, R. B., Jobbágy, E. G., Avissar, R., Roy, S. B., Barrett, D. J., Cook, C. W., Farley, K. A., Le Maitre, D. C., McCarl, B. A., & Murray, B. C. (2005). Atmospheric science: Trading water for carbon with biological carbon sequestration. *Science*, *310*(5756), 1944–1947. https://doi.org/10.1126/science.1119282

Jackson, R. B., Jobbágy, E. G., & Nosetto, M. D. (2009). Ecohydrology in a human-dominated landscape. *Ecohydrology*, *2*(3), 383–389. https://doi.org/10.1002/eco.81

Jeffrey, S. J., Carter, J. O., Moodie, K. B., & Beswick, A. R. (2001). Using spatial interpolation to construct a comprehensive archive of Australian climate data. *Environmental Modelling and Software*, *16*(4), 309–330. https://doi.org/10.1016/S1364-8152(01)00008-1

Jolly, I. D., Williamson, D. R., Gilfedder, M., Walker, G. R., Morton, R., Robinson, G., Jones, H., Zhang, L., Dowling, T. I., Dyce, P., Nathan, R. J., Nandakumar, N., Clarke, R., & McNeill, V. (2001). Historical stream salinity trends and catchment salt balances in the Murray-Darling basin, Australia. *Marine and Freshwater Research*, *52*(1), 53. https://doi.org/10.1071/MF00018

Li, H., Zhang, Y., Vaze, J., & Wang, B. (2012). Separating effects of vegetation change and climate variability using hydrological modelling and sensitivity-based approaches. *Journal of Hydrology*, *420–421*, 403–418. https://doi.org/10.1016/j.jhydrol.2011.12.033

Lundblad, M., & Lindroth, A. (2002). Stand transpiration and sapflow density in relation to weather, soil moisture and stand characteristics. *Basic and Applied Ecology*, *3*(3), 229–243. https://doi.org/10.1078/1439-1791-00099

Macfarlane, C., White, D. A., & Adams, M. A. (2004). The apparent feed-forward response to vapour pressure deficit of stomata in droughted, field-grown *Eucalyptus globulus* Labill. *Plant, Cell and Environment*, *27*(10), 1268–1280. https://doi.org/10.1111/j.1365-3040.2004.01234.x

Macinnis-ng, C. M. O., Zeppel, M. J. B., Palmer, A. R., & Eamus, D. (2016). Seasonal variations in tree water use and physiology correlate with soil salinity and soil water content in remnant woodlands on saline soils. *Journal of Arid Environments*, *129*, 102–110. https://doi.org/10.1016/j.jaridenv.2016.02.011

Marchionni, V., Guyot, A., Tapper, N., Walker, J. P., & Daly, E. (2019). Water balance and tree water use dynamics in remnant urban reserves. *Journal of Hydrology*, *575*(May), 343–353. https://doi.org/10.1016/j.jhydrol.2019.05.022

Marshall, D. C. (1958). Measurement of sap flow in conifers by heat transport. *Plant Physiology*, *33*(6), 385 LP – 396. https://doi.org/10.1104/pp.33.6.385

McCaskill, M. R., Raeside, M. C., Clark, S. G., Macdonald, C., Clark, B., & Partington, D. L. (2016). Pasture mixes with lucerne (*Medicago sativa*) increase yields and water-use efficiencies over traditional pastures based on subterranean clover (*Trifolium subterraneum*). *Crop and Pasture Science*, *67*(1), 69–80. https://doi.org/10.1071/CP14179

Meddings, R. L. A., McComb, J. A., Bell, D. T., Journal, A., & Agriculture, E. (2001). The salt-waterlogging tolerance of *Eucalyptus camaldulensis* x *E. globulus* hybrids. *Australian Journal of Experimental Agriculture*, *41*(6), 787–792.

Morand, V. J., Wohlt, K. E., Cayley, R. A., Taylor, D. H., Kemp, A. I. S., Simons, B. A., & Magart, A. P. M. (2003). Glenelg special map area geological report.

Niedda, M., & Pirastru, M. (2014). Field investigation and modelling of coupled stream discharge and shallow water-table dynamics in a small Mediterranean catchment (Sardinia). *Hydrological Processes*, *28*(21), 5423–5435. https://doi.org/10.1002/hyp.10016

Nosetto, M. D., Jobbágy, E. G., Tóth, T., & Jackson, R. B. (2008). Regional patterns and controls of ecosystem salinization with grassland afforestation along a rainfall gradient. *Global Biogeochemical Cycles*, *22*(2), 1–12. https://doi.org/10.1029/2007GB003000

O'Grady, A. P., Worledge, D., & Battaglia, M. (2008). Constraints on transpiration of *Eucalyptus globulus* in southern Tasmania, Australia. *Agricultural and Forest Meteorology*, *148*(3), 453–465. https://doi.org/10.1016/j.agrformet.2007.10.006

Pereira, J. S., Tenhunen, J. D., & Lange, O. L. (1987). Stomatal control of photosynthesis of *Eucalyptus globulus* labill. Trees under field conditions in Portugal. *Journal of Experimental Botany*, *38*(10), 1678–1688. https://doi.org/10.1093/jxb/38.10.1678

Peterson, T. J., Saft, M., Peel, M. C., & John, A. (2021). Watersheds may not recover from drought. *Science*, *372*(6543), 745–749. https://doi.org/10.1126/science.abd5085

Prăvălie, R. (2016). Drylands extent and environmental issues: A global approach. *Earth-Science Reviews*, *161*, 259–278. https://doi.org/10.1016/j.earscirev.2016.08.003

Scanlon, B. R., Jolly, I., Sophocleous, M., & Zhang, L. (2007). Global impacts of conversions from natural to agricultural ecosystems on water resources: Quantity versus quality. *Water Resources Research*, *43*(3), W03437. https://doi.org/10.1029/2006WR005486

Schlesinger, W. H., & Jasechko, S. (2014). Transpiration in the global water cycle. *Agricultural and Forest Meteorology*, *189–190*, 115–117. https://doi.org/10.1016/j.agrformet.2014.01.011

Sena Gomes, A. R., & Kozlowski, T. T. (1980). Effects of flooding on *Eucalyptus camaldulensis* and *Eucalyptus globulus* seedlings. *Oecologia*, *46*(2), 139–142. https://doi.org/10.1007/BF00540117

Silva, M. R. F., McHugh, I., Peixoto Neto, A. M. L., Pauwels, V. R. N., Cartwright, I., & Daly, E. (2022). Trading a little water for substantial carbon gains during the first years of a *Eucalyptus globulus* plantation. *Agricultural and Forest Meteorology*, *318*, 108910. https://doi.org/10.1016/j.agrformet.2022.108910

Silveira, L., Gamazo, P., Alonso, J., & Martínez, L. (2016). Effects of afforestation on groundwater recharge and water budgets in the western region of Uruguay. *Hydrological Processes*, *30*(20), 3596–3608. https://doi.org/10.1002/hyp.10952

Steppe, K., De Pauw, D. J. W., Doody, T. M., & Teskey, R. O. (2010). A comparison of sap flux density using thermal dissipation, heat pulse velocity and heat field deformation methods. *Agricultural and Forest Meteorology*, *150*(7–8), 1046–1056. https://doi.org/10.1016/j.agrformet.2010.04.004

Thayalakumaran, T., McCaskill, M., & Morse-McNabb, E. M. (2018). Estimating soil water in high-rainfall zones under pasture. *Agricultural Systems*, *165*, 252–263. https://doi.org/10.1016/j.agsy.2018.06.019

Van Dijk, A. I. J. M., Beck, H. E., Crosbie, R. S., De Jeu, R. A. M., Liu, Y. Y., Podger, G. M., Timbal, B., & Viney, N. R. (2013). The millennium drought in Southeast Australia (2001-2009): Natural and human causes and implications for water resources, ecosystems, economy, and society. *Water Resources Research*, *49*(2), 1040–1057. https://doi.org/10.1002/wrcr.20123

van Dijk, A. I. J. M., & Keenan, R. J. (2007). Planted forests and water in perspective. *Forest Ecology and Management*, *251*(1–2), 1–9. https://doi.org/10.1016/j.foreco.2007.06.010

Vandegehuchte, M. W., & Steppe, K. (2013). Sap-flux density measurement methods: Working principles and applicability. *Functional Plant Biology*, *40*(3), 213–223. https://doi.org/10.1071/FP12233

Veldkamp, T. I. E., Wada, Y., Aerts, J. C. J. H., Döll, P., Gosling, S. N., Liu, J., Masaki, Y., Oki, T., Ostberg, S., Pokhrel, Y., Satoh, Y., Kim, H., & Ward, P. J. (2017). Water scarcity hotspots travel downstream due to human interventions in the 20th and 21st century. *Nature Communications*, *8*(1), 1–12. https://doi.org/10.1038/ncomms15697

Ward, P. R., & Dunin, F. X. (2001). Growing season evapotranspiration from duplex soils in South-Western Australia. *Agricultural Water Management*, *50*(2), 141–159. https://doi.org/10.1016/S0378-3774(01)00092-0

Webb, A. A., & Kathuria, A. (2012). Response of streamflow to afforestation and thinning at Red Hill, Murray Darling basin, Australia. *Journal of Hydrology*, *412–413*, 133–140. https://doi.org/10.1016/j.jhydrol.2011.05.033

Whitley, R., Taylor, D., Macinnis-Ng, C., Zeppel, M., Yunusa, I., O'Grady, A., Froend, R., Medlyn, B., & Eamus, D. (2013). Developing an empirical model of canopy water flux describing the common response of transpiration to solar radiation and VPD across five contrasting woodlands and forests. *Hydrological Processes*, *27*(8), 1133–1146. https://doi.org/10.1002/hyp.9280

Zeppel, M., Macinnis-Ng, C. M. O., Ford, C. R., & Eamus, D. (2008). The response of sap flow to pulses of rain in a temperate Australian woodland. *Plant and Soil*, *305*(1–2), 121–130. https://doi.org/10.1007/s11104-007-9349-7

Zeppel, M. J. B., Murray, B. R., Barton, C., & Eamus, D. (2004). Seasonal responses of xylem sap velocity to VPD and solar radiation during drought in a stand of native trees in temperate Australia. *Functional Plant Biology*, *31*(5), 461–470. https://doi.org/10.1071/FP03220

Zhang, L., Vertessy, R., Walker, G., Gilfedder, M., & Hairsine, P. (2007). Afforestation in a catchment context. Industry report *1/07* (01): 1–60.

Zhang, L., Zhao, F., Chen, Y., & Dixon, R. N. M. (2011). Estimating effects of plantation expansion and climate variability on streamflow for catchments in Australia. *Water Resources Research*, *47*(12), W12539. https://doi.org/10.1029/2011WR010711

Zhang, L., Zhao, F. F., & Brown, A. E. (2012). Predicting effects of plantation expansion on streamflow regime for catchments in Australia. *Hydrology and Earth System Sciences*, *16*(7), 2109–2121. https://doi.org/10.5194/hess-16-2109-2012

Zhang, M., Liu, N., Harper, R., Li, Q., Liu, K., Wei, X., Ning, D., Hou, Y., & Liu, S. (2017). A global review on hydrological responses to forest change across multiple spatial scales: Importance of scale, climate, forest type and hydrological regime. *Journal of Hydrology*, *546*, 44–59. https://doi.org/10.1016/j.jhydrol.2016.12.040

How to cite this article: Peixoto Neto, A. M. L., Cartwright, I., Silva, M. R. F., McHugh, I., Dresel, P. E., Teodosio, B., Jovanovic, D., McCaskill, M. R., Webb, J., & Daly, E. (2022). Linking evapotranspiration seasonal cycles to the water balance of headwater catchments with contrasting land uses. *Hydrological Processes*, *36*(12), e14784. https://doi.org/10.1002/hyp.14784